Chemical Science

ROYAL SOCIETY OF CHEMISTRY

EDGE ARTICLE

Check for updates

Cite this: *Chem. Sci.*, 2023, **14**, 10884

All publication charges for this article have been paid for by the Royal Society of Chemistry

Received 19th July 2023
Accepted 12th September 2023

DOI: 10.1039/d3sc03719c

rsc.li/chemical-science

Photo-caged 2-butene-1,4-dial as an efficient, target-specific photo-crosslinker for covalent trapping of DNA-binding proteins†‡

Jiahui Li, Zenghui Cui, Chaochao Fan, Yifei Zhou, Mengtian Ren and Chuanzheng Zhou *

Covalent trapping of DNA-binding proteins *via* photo-crosslinking is an advantageous method for studying DNA–protein interactions. However, traditional photo-crosslinkers generate highly reactive intermediates that rapidly and non-selectively react with nearby functional groups, resulting in low target-capture yields and high non-target background capture. Herein, we report that photo-caged 2-butene-1,4-dial (PBDA) is an efficient photo-crosslinker for trapping DNA-binding proteins. Photo-irradiation (360 nm) of PBDA-modified DNA generates 2-butene-1,4-dial (BDA), a small, long-lived intermediate that reacts selectively with Lys residues of DNA-binding proteins, leading in minutes to stable DNA–protein crosslinks in up to 70% yield. In addition, BDA exhibits high specificity for target proteins, leading to low non-target background capture. The high photo-crosslinking yield and target specificity make PBDA a powerful tool for studying DNA–protein interactions.

Introduction

The maintenance and function of DNA in cells depend on its interactions with various proteins, including but not limited to histones,[1] epigenetic writer/reader/eraser proteins,[2] DNA repair enzymes,[3] and transcription factors.[4] DNA–protein interactions are generally non-covalent and transient, and therefore the identification of DNA-binding proteins by many of the routinely used technologies is tedious and difficult.[5] Photo-crosslinkers have attracted considerable attention as a potential solution to this problem.[6,7] Photo-irradiation of DNA modified with a photo-crosslinker can covalently trap DNA-binding proteins, thus making it possible to lock transient interactions with high spatiotemporal resolution *in vitro* and *in vivo*.[8–12] To date, three types of photo-crosslinkers have been extensively used for this purpose: aryl azides (AA), benzophenones (BP), and diazirines (DA) (Fig. 1A).[13,14] However, photo-irradiation of these compounds generates highly reactive intermediates that react non-selectively with nearby functional groups, resulting in low target-capture yields and high non-target background capture.[15] Although several new photo-crosslinkers,[13] including 2-aryl-5-carboxytetrazole,[16,17] photo-caged quinone methide,[18] and *o*-nitrobenzyl alcohol,[19] exhibit interesting features, the development of photo-crosslinkers that can trap DNA-binding proteins with both high specificity and high yield remains a challenge.

DNA-binding proteins are generally rich in Lys residues,[20] and modifying DNA with Lys-reactive functionality has been

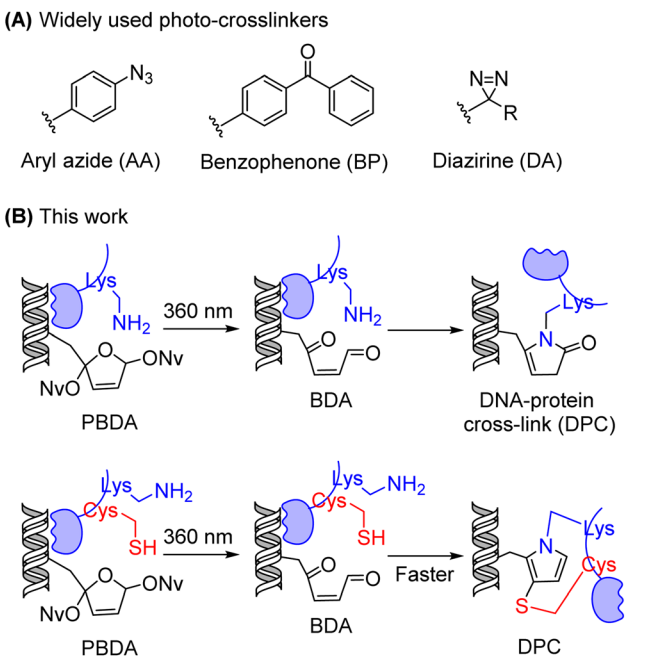

Fig. 1 Structures of photo-crosslinkers used to study DNA–protein interactions.

State Key Laboratory of Elemento-Organic Chemistry, Frontiers Science Center for New Organic Matter, Department of Chemical Biology, College of Chemistry, Nankai University, Tianjin 300071, China. E-mail: chuanzheng.zhou@nankai.edu.cn

† Dedication to Professor Zhen Xi on the occasion of his 60th birthday.

‡ Electronic supplementary information (ESI) available: General experimental methods, spectroscopic data and supplementary figures and tables (PDF). See DOI: https://doi.org/10.1039/d3sc03719c

This article is licensed under a Creative Commons Attribution-NonCommercial 3.0 Unported Licence.

(cc) BY-NC

© 2023 The Author(s). Published by the Royal Society of Chemistry

reported as a new strategy for trapping DNA-binding proteins.[19,21–23] We have previously demonstrated that a C4′-oxidized abasic site (C4-AP) reacts with primary amines to form stable conjugates.[24–28] In the present study, we designed and synthesized an analogue of C4-AP, photo-caged 2-butene-1,4-dial (PBDA, Fig. 1B), as a new photo-crosslinker for identifying DNA-binding proteins. The irradiation (360 nm) of this crosslinker generates 2-butene-1,4-dial (BDA),[29–33] a small, relatively long-lived intermediate that reacts selectively with Lys residues on DNA-binding proteins, leading to stable DNA–protein crosslinks in yields up to 70%. If there is a Cys residue close to the Lys, the Cys can participate in and speed up crosslink formation.

Results and discussion

Synthesis of PBDA

As a versatile tool for introducing the PBDA moiety into DNA, we designed and synthesized azide **1**, which can be used for post-synthetic labeling of DNA *via* click chemistry (Scheme 1A). The synthesis of **1** started from 2-furanethanol (**2**). The hydroxyl group of **2** was protected as a *t*-butyldiphenylsilyl ether, and the resulting ether compound (**3**) could be treated either with 4,5-dimethoxy-2-nitrobenzyl alcohol in the presence of *N*-bromosuccinimide[34] or with 2,3-dichloro-5,6-dicyanobenzoquinone[35,36] to afford photo-caged compound **4** in 55% or 28% yield, respectively. After removal of the *t*-butyldiphenylsilyl protecting group, the resulting alcohol was converted to an azide by treatment with 2-azido-1,3-dimethylimidazolinium hexafluorophosphate in the presence of diazabicycloundecene to afford **1** in 63% yield. Using the same strategy, we also synthesized PBDA analogue **7** (Scheme 1B), which was used for assessing the reactivity of PBDA with model peptides.

Mechanistic study of photo-reactions of PBDA analogue 7 with model peptides

To characterize the reactivity of PBDA with amino acids, we photo-irradiated **7** at 365 nm in the presence of glycinamide, which removed the Nv protecting group to generate intermediate **8** (Fig. 2A). This intermediate could be detected by ultra-performance liquid chromatography mass spectrometry (UPLC-MS), suggesting that it was long-lived. Ring-opening of **8** in aqueous solution afforded highly electrophilic BDA **9**, which reacted with glycinamide to give pyrrolinone adduct **10** as the predominant product. Similarly, photo-irradiation of **7** in the presence of $BnNH_2$ gave pyrrolinone adduct **11**. In contrast, photo-irradiation of **7** in the presence of $BnNH_2$ and 2-mercaptoethanol yielded pyrrole adduct **12** as the predominant product (Fig. S1‡). Because the nitrogen atom in **12** is a chiral center, two stable isomers were formed (**12-I** and **12-II**), and they could be separated into their pure forms. Pyrrolinone adduct **10** and pyrrole adducts **12-I** and **12-II** were unambiguously characterized by means of various one- and two-dimensional NMR spectroscopy techniques (see the ESI‡). Neither **10** nor **12-II** decomposed when incubated for 12 h in neutral, acidic, or basic buffers, suggesting that both adducts were stable (Fig. S2‡). Of note, photo-irradiation of **7** generates another active electrophile, 4,5-dimethoxy-2-nitrosobenzaldehyde (Fig. 2A), which could also react with amines. However, we did not observe side products formed by the reaction of 4,5-dimethoxy-2-nitrosobenzaldehyde with glycinamide/$BnNH_2$. Thus, BDA outcompetes 4,5-dimethoxy-2-nitrosobenzaldehyde on reacting with amines. We think two factors may account for the result: first, 4,5-dimethoxy-2-nitrosobenzaldehyde, as an aromatic aldehyde, is much less electrophilic than the aliphatic aldehyde BDA **9**;[37] Second, the reaction of 4,5-dimethoxy-2-nitrosobenzaldehyde with amines is reversible, affording unstable products.[38] In contrast, the reaction of BDA with amines generates rather stable products.

Next, we designed and carried out experiments to assess the reactivity of **7** with polypeptides **13**, **16**, and **19** (Fig. 2B–D). After a mixture of peptide **13** and **7** (1.5 equiv.) in phosphate buffer (pH 7.4) was irradiated and then incubated for 20 min, UPLC-MS showed that roughly 40% of peptide **13** had been transformed to a pyrrolinone monoadduct with an *m*/*z* value of 961.9285 ($[M + 2H]^{2+}$, Fig. 2B). MS/MS analysis of the adduct

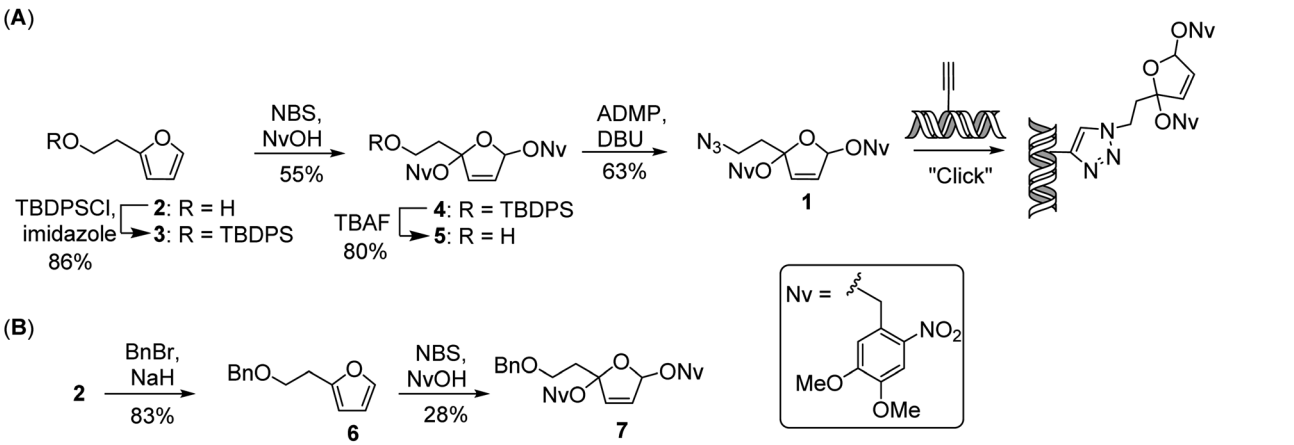

Scheme 1 Synthesis of (A) PBDA and (B) analogue **7**. ADMP, 2-azido-1,3-dimethylimidazolinium hexafluorophosphate; Bn, benzyl; DBU, diazabicycloundecene; NBS, *N*-bromosuccinimide; NvOH, 4,5-dimethoxy-2-nitrobenzyl alcohol; TBDPS, *t*-butyldiphenylsilyl.

© 2023 The Author(s). Published by the Royal Society of Chemistry

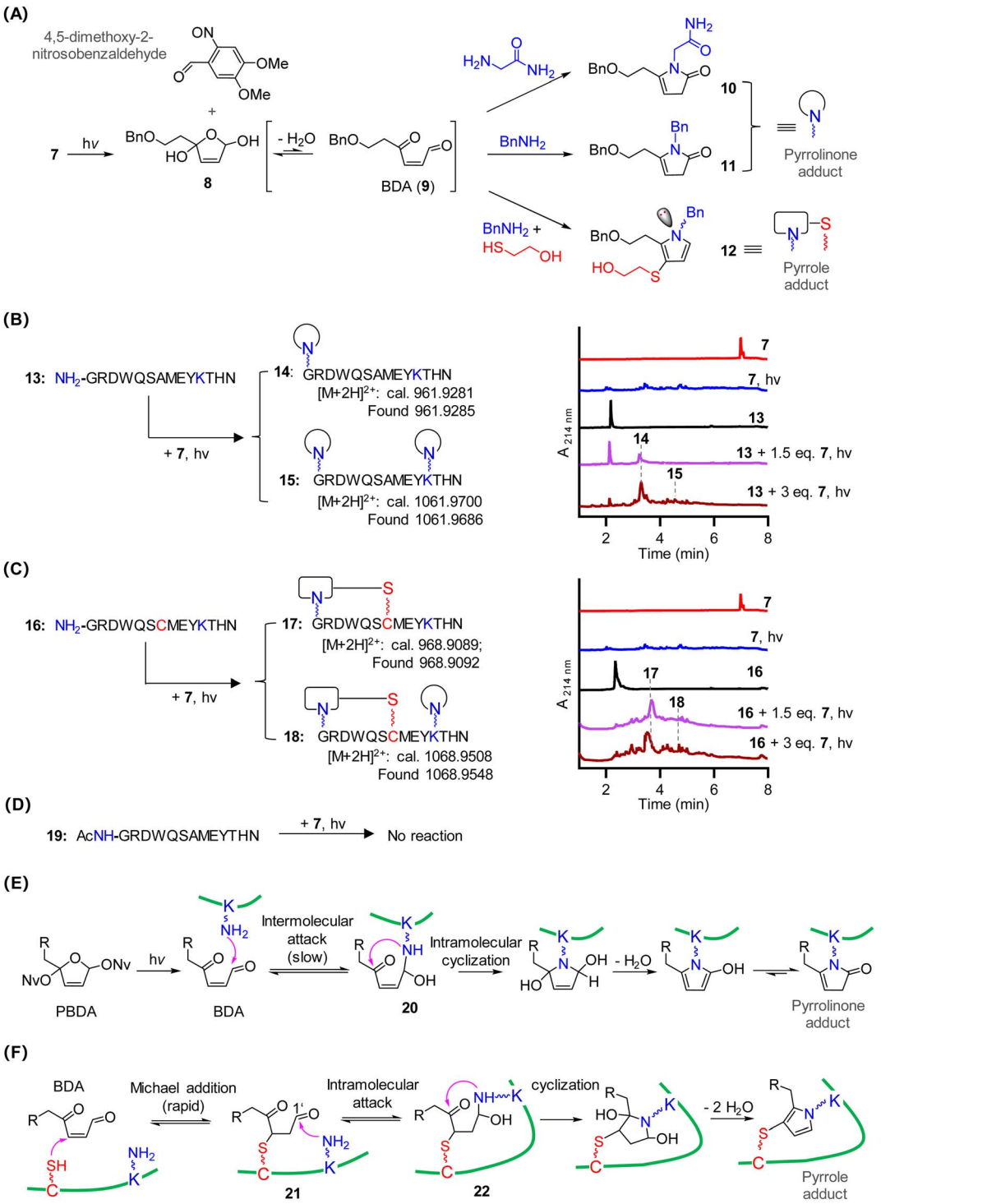

Fig. 2 Mechanistic studies of photo-reactions of PBDA analogue **7** with amino acids and peptides. (A) Photo-reactions of **7** with amines and thiols. (B–D) UPLC-MS analyses of photo-reactions of **7** with various peptides. (E) Proposed mechanism of photo-reaction of **7** with a Lys residue. (F) Proposed mechanism for photo-reaction of **7** with Cys and Lys residues.

revealed that the pyrrolinone moiety was on the N-terminal α-amino group (**14**, Fig. S3‡). Increasing the amount of **7** to 3 equiv. led to the formation of adduct **15**, which had pyrrolinone moieties both on the ε-amino group of the Lys residue and on the N-terminal α-amino group (Fig. S4‡). These results indicate that the α-amino group was more reactive than the Lys side chain, which is consistent with previous observations that N-terminal α-amino groups outcompete the ε-amino group of Lys in reactions with electrophiles in neutral buffer.[39,40]

The incubation of peptide **16**, which has Cys instead of Ala at position 7, with 1.5 equiv. of **7** completely transformed **16** to cyclic pyrrole adduct **17** in 20 min (Fig. 2C and S5‡). This result

© 2023 The Author(s). Published by the Royal Society of Chemistry

suggests that the formation of the Cys-involved pyrrole adduct was much faster than pyrrolinone adduct formation. Product **18** (calc m/z of $[M + 2H]^{2+}$, 1068.9508; found 1068.9548), which contains both a pyrrole adduct and a pyrrolinone adduct (Fig. S6‡), was obtained when the amount of **7** was increased to 3 equiv.

No reaction occurred upon photo-irradiation of a mixture of **7** and peptide **19** which contains no Cys, Lys, and free N-terminal α-amino functional groups (Fig. 2D and S7‡). In addition, the reaction of photo-decaged **7** with a peptide containing one Cys reside but no Lys residues and no free N-terminal α-amino group also proceeded smoothly, but no stable product could be isolated, indicating that reversible crosslinks could be formed (data not shown).

On the basis of the above-described results and our previous work on peptides with a C4′-oxidized abasic site (BDA analogues),[24–27] we propose the following mechanism for the reaction of PBDA with peptides. For peptides containing Lys but not Cys, the ε-amino group of Lys reacts with BDA to afford **20**. Once **20** forms, intramolecular cyclization and elimination of water occur to generate a pyrrolinone adduct (Fig. 2E). For peptides containing both Cys and Lys, Michael addition of Cys to BDA to generate **21** is much more rapid than the reaction between BDA and the ε-amine group of Lys.[41,42] After the formation of **21**, the Lys ε-amino group intramolecularly attacks the C1′ aldehyde to generate intermediate **22**. The subsequent cyclization and elimination of water afford a pyrrole adduct (Fig. 2F). For peptides with a Cys residue but no Lys residue and free N-terminal α-amino group, the adduct formed by reaction between Cys and BDA is not stable, and decomposition occurs *via* the retro-Michael addition reaction. Taken together, our results indicate that PBDA is a Lys-specific photo-crosslinker and that a Cys residue near Lys can speed up crosslink formation.

Intramolecular photo-crosslinking of PBDA-modified DNA with histones in nucleosome core particles

Nucleosome core particles (NCPs), the fundamental unit of chromatin, are compact and stable DNA–histone complexes.[1] We prepared PBDA-modified NCPs as intramolecular models for optimizing the conditions for photo-crosslinking of PBDA with DNA-binding proteins. Specifically, single-stranded DNA with a 5-ethynyl-2′-deoxyuridine (ethynyl-dU), 5-(1,7-octadiynyl)-2′-deoxyuridine (octadiynyl-dU), or 1′-propargyl-2′-deoxyribose (propargyl-ribo) modification was coupled with PBDA (**1**) in the presence of Cu(I), and the obtained product was annealed with the complementary DNA strand to afford PBDA-modified double-stranded DNA (dsDNA). Finally, PBDA-modified NCPs were prepared by reconstitution of the modified dsDNA with a histone octamer (Fig. 3A, S8, and S9, Table S1‡).[28,39,43]

PBDA-modified NCPs were irradiated for various durations, and the DNA–histone crosslink yields were quantified by SDS-PAGE (Fig. S10‡). As shown in Fig. 3B, photo-crosslinking of PBDA to histones was clearly affected by the nature of the linker between the DNA strand and the PBDA moiety. The most flexible linker (the 1,7-octadiynyl linker) gave the best results: the DNA–histone crosslink yield reached 70% within 2 min.

The flexible N-terminal tails of histones H3 and H4 are in proximity to the PBDA-octadiynyl-dU moiety on the NCPs (Fig. 3C), and these histone tails contain many Lys residues but no Cys.[44] Thus, we reasoned that DNA–histone crosslinking occurred *via* the formation of pyrrolinone adducts between photo-decaged PBDA and Lys residues on these histone tails. After photo-crosslink formation, further incubation of the reaction mixture for up to 12 h resulted in no changes in the crosslink yields (Fig. S11‡), confirming that PBDA-modified-DNA–protein crosslinks were stable.

To compare the photo-crosslinking efficiency of PBDA with that of widely used photo-crosslinkers, we prepared benzophenones (BP)-octadiynyl-dU- and diazirine (DA)-octadiynyl-dU-modified NCPs and studied their photo-crosslinking kinetics. Photo-crosslinking of DA to histones within NCPs was rapid, yielding DNA–histone crosslinking in up to 15% yield within 3 min (Fig. 3D and S12‡). Photo-crosslinking of BP to histones occurred more slowly but gave a slightly higher crosslinking yield, reaching a plateau (30%) at 20 min (Fig. S12‡). Under the same conditions, PBDA yielded 70% DNA–histone crosslinking in 2 min. Taken together, PBDA is more rapid and efficient than classical photo-crosslinkers for the covalent trapping of DNA-binding proteins.

Intermolecular photo-crosslinking of PBDA-modified DNA with DNA-binding proteins

Because the above-described results demonstrated that PBDA-octadiynyl-dU was an excellent photo-crosslinker, rapidly yielding DNA–protein crosslinks (>70% yield) in DNA–protein complexes, we next prepared dsDNA **26** (Fig. 4A), which was modified with both PBDA-octadiynyl-dU and 5-formyl-2′-deoxycytidine (5fC), an epigenetic modification that can be recognized and removed by the base excision repair enzyme thymine DNA glycosylase (TDG, Fig. 4B).[45,46] Once prepared, dsDNA **26** was used as a substrate to study intermolecular photo-crosslinking of DNA with a DNA-binding protein. Specifically, **26** was preincubated with 10 equiv. of human TDG and bovine serum albumin (BSA, 0.05 mg mL^{-1}, Fig. S13‡), and the mixture was photo-irradiated for 7 min. Tricine-SDS-PAGE analysis of the reaction mixture showed a DNA–TDG crosslink yield of 63% (Fig. 4C, lane 4). No DNA–BSA crosslinks (Fig. 4C, lane 2 and Fig. S14‡) or DNA interstrand crosslinks (Fig. S15‡) were observed. Two pathways can account for the DNA–TDG crosslinking: (1) the formation of C=N bonds between the formyl group of 5fC and Lys residues on TDG[39] and (2) the reactions of photo-decaged PBDA with Lys (and Cys) on TDG. We concluded that the contribution of the former pathway was negligible, because dsDNA–TDG crosslinking was negligible in the absence of photo-irradiation (Fig. 4C, lane 3).

When dsDNA **27** or **28**, in which the PBDA-octadiynyl-dU modification is farther from the TDG-binding region, was used as the substrate, decreased crosslink yields were observed (Fig. 4C). TDG has been shown to have less binding affinity for native dsDNA than for 5fC-modified dsDNA.[46] Consistent with this fact, we found that the crosslink yield for the combination of TDG and dsDNA **29** (which does not contain 5fC) was clearly

© 2023 The Author(s). Published by the Royal Society of Chemistry

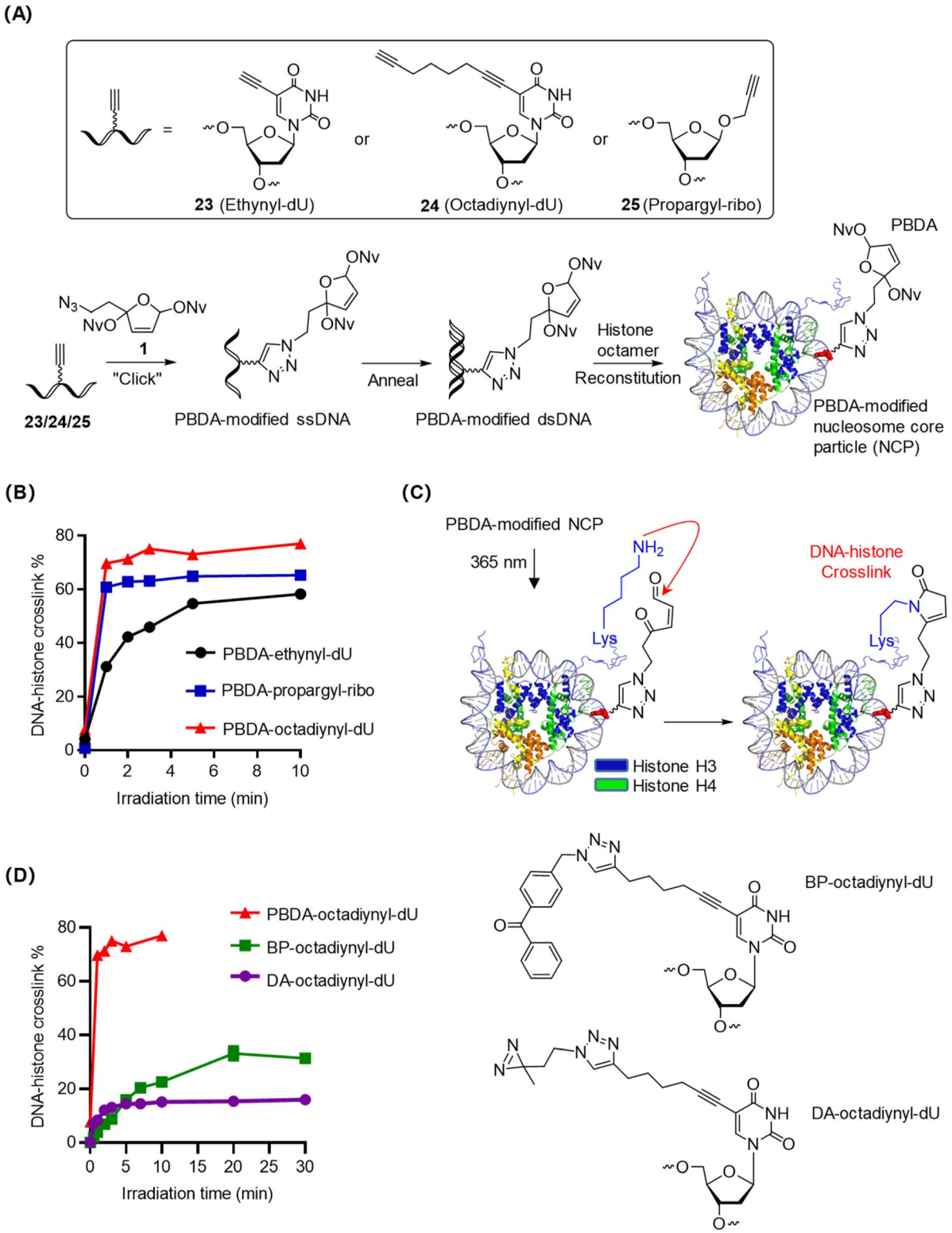

Fig. 3 Photo-crosslinking of PBDA-modified DNA with histones within NCPs. (A) Preparation of PBDA-modified NCPs. ssDNA, single-stranded DNA. (B) Kinetics of photo-crosslinking of PBDA-modified DNA to histones within NCPs. (C) Proposed mechanism of photo-crosslinking of PBDA-modified DNA to histones within NCPs. (D) Comparison of the photo-crosslinking kinetics of PBDA with that of BP and DA within NCPs.

© 2023 The Author(s). Published by the Royal Society of Chemistry

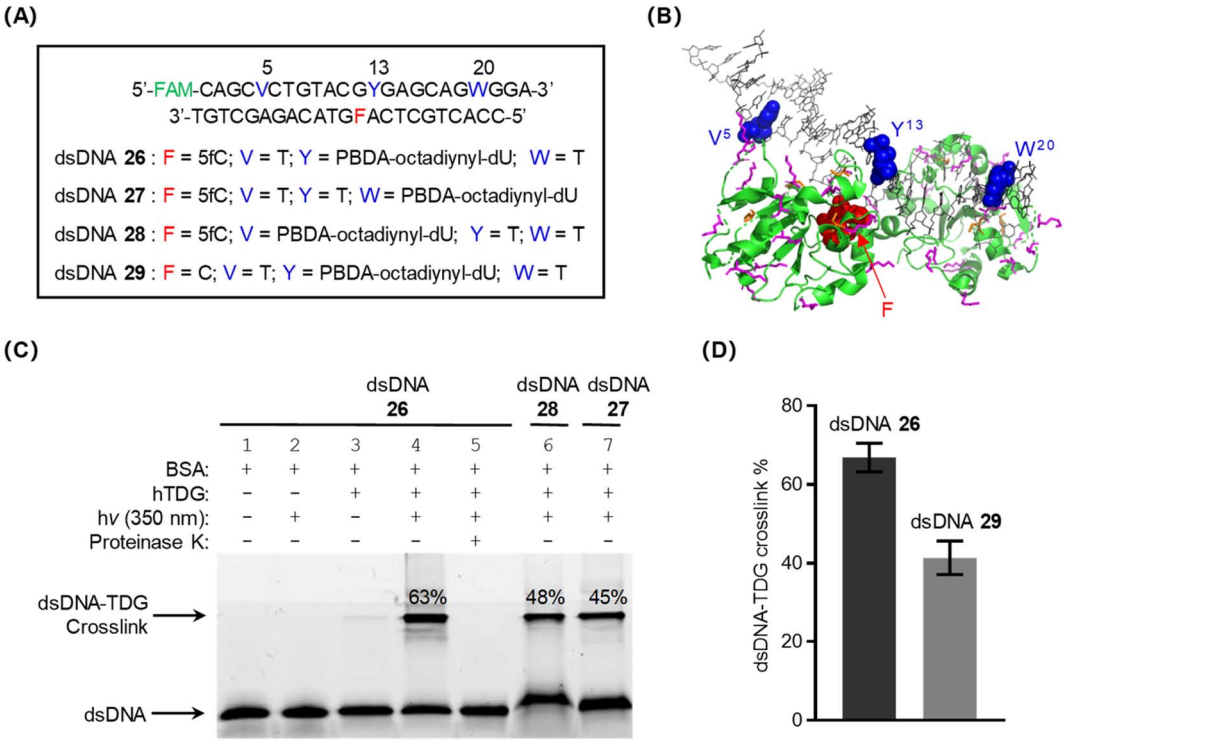

Fig. 4 Intermolecular photo-crosslinking of PBDA-modified DNA with the DNA base excision repair enzyme hTDG. (A) PBDA-octadiynyl-dU- and 5fC-modified dsDNA used in this study. (B) Crystal structure of the dsDNA–TDG complex (PDB ID: 3UO7). The PBDA-octadiynyl-dU and 5fC modification sites are indicated by blue and red spheres, respectively. Lys residues and Cys residues are indicated by pink and orange sticks, respectively. (C) Tricine-SDS-PAGE (15.5%) analysis of photo-crosslinking of dsDNA with TDG. The gel was visualized by means of fluorescence (fluorescein, FAM) imaging. BSA, bovine serum albumin. (D) Comparison of photo-crosslink yields for dsDNA **26** and dsDNA **29**.

lower than that for the TDG/dsDNA **26** combination (Fig. 4D and S16‡). These results confirm that PBDA is an excellent photo-crosslinker for covalently trapping DNA-binding proteins and that it exhibits rather good specificity for target protein.

Pull down of DNA-binding proteins from cell lysate using PBDA-modified DNA

Escherichia coli cells that overexpress human TDG were harvested, lysed, and centrifuged; and the supernatant was collected for a pull-down assay. Because of serious sedimentation, the concentration of expressed human TDG in the supernatant was very close to the concentrations of the endogenous proteins of *E. coli* (Fig. 5, lane 5), making this supernatant an ideal sample for determining whether 5fC- and PBDA-modified dsDNA **30** could be used to pull down hTDG from a protein mixture *via* photo-crosslinking.

Biotinylated dsDNA **30** and cell lysate were mixed and incubated at 4 °C for 2.5 h to allow for DNA–protein binding. After photo-irradiation for 7 min, the mixture was incubated at 37 °C for 30 min (Fig. 5, lane 6). Then streptavidin-coated magnetic beads were added to capture the biotinylated dsDNA. After removal of the supernatant (lane 7), the beads were successively washed with 1 M NaCl, 0.1% SDS, 6 M urea, and phosphate-buffered saline. Finally, the trapped DNA and the crosslinked DNA–protein complexes were eluted with SDS loading buffer at 70 °C and analyzed with 15% SDS-PAGE (Fig. 5, lane 8). The major product was identified as crosslinked DNA–TDG on the basis of the following observations: (1) the product co-migrated with the authentic sample of DNA–TDG in the gel (Fig. 5, lane

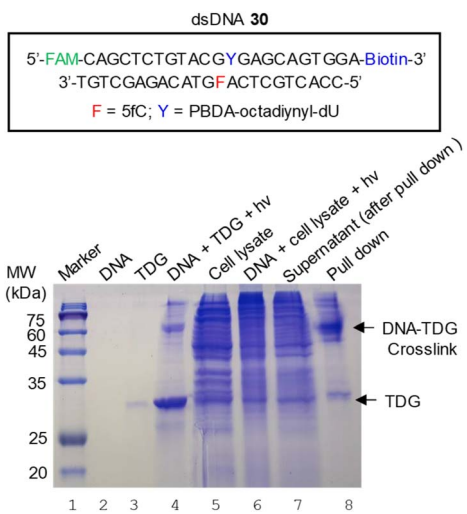

Fig. 5 Pull down of TDG from cell lysate using PBDA-modified dsDNA **30**. TDG-containing cell lysate was mixed with biotinylated dsDNA **30**, and the mixture was subjected to photolysis. After incubation for 30 min, the biotinylated DNA was pulled down using streptavidin-coated magnetic beads. After a harsh wash, the captured molecules were eluted with SDS loading buffer and analyzed with 15% SDS-PAGE. The gel in the image was stained with Coomassie brilliant blue.

© 2023 The Author(s). Published by the Royal Society of Chemistry

4); (2) the band was visible during fluorescence imaging (Fig. S17A‡), which suggests that the product contained fluorescein-labeled dsDNA **30**; (3) the band was visible during anti-TDG western blot analysis (Fig. S17B‡), suggesting the presence of TDG; (4) in-gel trypsin digestion followed by MS/MS analysis revealed that hTDG was abundant in this band (Table S2‡). Of note, unexpected proteins were also identified by MS/MS. Some of them, such as human hornerin and serum albumin, could be contaminants introduced during sample handling,[47,48] whereas some others could be ascribed to non-specific trapping of DNA-binding proteins.

Conclusions

In this study, we demonstrated that PBDA is an efficient, target-specific photo-crosslinker for trapping and identification of DNA-binding proteins. Compared with traditional photo-crosslinkers such as aryl azide, benzophenone, and diazirine, PBDA has three obvious advantages. First, it gives higher crosslink yields (up to 70%). Two factors may account for the high yields: (i) the intermediate generated by photo-decaging of PBDA (BDA) is less reactive than radicals, carbenes, and nitrenes, and thus its background quenching is negligible, and (ii) the small size and linearity of BDA (*in situ* generated by photo-irradiation of PBDA) facilitate its approach to and reaction with DNA-binding proteins. Second, the photo-reaction of PBDA with DNA-binding proteins was Lys-specific and was complete in minutes. The high residue specificity and moderate reaction rate allowed photo-decaged PBDA to selectively trap target proteins, minimizing non-target background trapping. Third, given that MS/MS analysis has become the predominant method for protein identification, the Lys-specific reactivity of PBDA makes MS/MS data analysis less complicated than when a residue-nonspecific crosslinker is employed.

In addition to being abundant in nucleic-acid-binding proteins, Lys is present in almost all proteins, especially in regions with relatively high solvent accessibility.[49–51] Thus, PBDA may find broad applications for investigating RNA–protein and protein–protein interactions in addition to DNA–protein interactions.

Data availability

Experimental procedures and all relevant data are available in ESI‡ and from the authors.

Author contributions

J. L. and Z. C. performed the experiments. C. F., Y. Z. and M. R. provided guidance on some experimental details and contributed new reagents/analytic tools. C. Z. designed and supervised the project. The initial draft of the manuscript was written by J. Li and C. Z. All authors discussed the results and have given approval to the final version of the manuscript.

Conflicts of interest

There are no conflicts to declare.

Acknowledgements

This work was supported by the National Natural Science Foundation of China (no. 22377059 and 91953115), the Natural Science Foundation of Tianjin City (no. 20JCZDJC00830), and the Frontiers Science Center for New Organic Matter, Nankai University (no. 63181206).

Notes and references

1 R. K. McGinty and S. Tan, *Chem. Rev.*, 2015, **115**, 2255–2273.
2 R. Ren, J. R. Horton, X. Zhang, R. M. Blumenthal and X. Cheng, *Curr. Opin. Struct. Biol.*, 2018, **53**, 88–99.
3 N. C. Bauer, A. H. Corbett and P. W. Doetsch, *Nucleic Acids Res.*, 2015, **43**, 10083–10101.
4 D. Yesudhas, M. Batool, M. A. Anwar, S. Panneerselvam and S. Choi, *Genes*, 2017, **8**, 192.
5 M. F. Carey, C. L. Peterson and S. T. Smale, *Cold Spring Harb. Protoc.*, 2012, **1**, 18–33.
6 Y. Tian and Q. Lin, *Chimia*, 2018, **72**, 758–763.
7 G. W. Preston and A. J. Wilson, *Chem. Soc. Rev.*, 2013, **42**, 3289–3301.
8 J. J. Tate, J. Persinger and B. Bartholomew, *Nucleic Acids Res.*, 1998, **26**, 1421–1426.
9 U. K. Shigdel, J. L. Zhang and C. He, *Angew. Chem., Int. Ed.*, 2008, **47**, 90–93.
10 M. Winnacker, S. Breeger, R. Strasser and T. Carell, *ChemBioChem*, 2009, **10**, 109–118.
11 Y. Liu, W. Zheng, W. Zhang, N. Chen, Y. Liu, L. Chen, X. Zhou, X. Chen, H. Zheng and X. Li, *Chem. Sci.*, 2015, **6**, 745–751.
12 J. Zhang, J. Peng, Y. Huang, L. Meng, Q. Li, F. Xiong and X. Li, *Angew. Chem., Int. Ed.*, 2020, **59**, 17525–17532.
13 J. P. Holland, M. Gut, S. Klingler, R. Fay and A. Guillou, *Chem.–Eur. J.*, 2020, **26**, 33–48.
14 M. M. Hassan and O. O. Olaoye, *Molecules*, 2020, **25**, 2285.
15 P. Kleiner, W. Heydenreuter, M. Stahl, V. S. Korotkov and S. A. Sieber, *Angew. Chem., Int. Ed.*, 2017, **56**, 1396–1401.
16 A. Herner, J. Marjanovic, T. M. Lewandowski, V. Marin, M. Patterson, L. Miesbauer, D. Ready, J. Williams, A. Vasudevan and Q. Lin, *J. Am. Chem. Soc.*, 2016, **138**, 14609–14615.
17 Y. Tian, M. P. Jacinto, Y. Zeng, Z. Yu, J. Qu, W. R. Liu and Q. Lin, *J. Am. Chem. Soc.*, 2017, **139**, 6078–6081.
18 J. Liu, L. Cai, W. Sun, R. Cheng, N. Wang, L. Jin, S. Rozovsky, I. B. Seiple and L. Wang, *Angew. Chem., Int. Ed.*, 2019, **58**, 18839–18843.
19 W. Hu, Y. Yuan, C.-H. Wang, H.-T. Tian, A.-D. Guo, H.-J. Nie, H. Hu, M. Tan, Z. Tang and X.-H. Chen, *Chem*, 2019, **5**, 2955–2968.
20 J. Zhang, Z. Ma and L. Kurgan, *Briefings Bioinf.*, 2019, **20**, 1250–1268.

© 2023 The Author(s). Published by the Royal Society of Chemistry

21 C. B. Rosen, L. B. KodalAnne, J. S. Nielsen, D. H. Schaffert, C. Scavenius, A. H. Okholm, N. V. Voigt, J. J. Enghild, J. Kjems, T. Tørring and K. V. Gothelf, *Nat. Chem.*, 2014, **6**, 804–809.
22 V. Raindlova, R. Pohl and M. Hocek, *Chem.–Eur. J.*, 2012, **18**, 4080–4087.
23 M. Hocek, *Acc. Chem. Res.*, 2019, **52**, 1730–1737.
24 C. Zang, H. Wang, T. Li, Y. Zhang, J. Li, M. Shang, J. Du, Z. Xi and C. Zhou, *Chem. Sci.*, 2019, **10**, 8973–8980.
25 Y. Zhang, X. Zhou, Y. Xie, M. M. Greenberg, Z. Xi and C. Zhou, *J. Am. Chem. Soc.*, 2017, **139**, 6146–6151.
26 C. Z. Zhou, J. T. Sczepanski and M. M. Greenberg, *J. Am. Chem. Soc.*, 2013, **135**, 5274–5277.
27 Y. Zhang, C. Zang, G. An, M. Shang, Z. Cui, G. Chen, Z. Xi and C. Zhou, *Nat. Commun.*, 2020, **11**, 1015.
28 M. Ren, M. M. Greenberg and C. Zhou, *Acc. Chem. Res.*, 2022, **55**, 1059–1073.
29 L. A. Peterson, *Chem. Res. Toxicol.*, 2013, **26**, 6–25.
30 J. Nunes, I. L. Martins, C. Charneira, I. P. Pogribny, A. de Conti, F. A. Beland, M. M. Marques, C. C. Jacob and A. M. M. Antunes, *Toxicol. Lett.*, 2016, **264**, 106–113.
31 L. L. G. Carrette, T. Morii and A. Madder, *Bioconjugate Chem.*, 2013, **24**, 2008–2014.
32 J. S. Jha, J. Yin, T. Haldar, Z. Yang, Y. Wang and K. S. Gates, *J. Am. Chem. Soc.*, 2022, **144**, 10471–10482.
33 A. Manicardi, E. Cadoni and A. Madder, *Chem. Sci.*, 2020, **11**, 11729–11739.
34 S. Caddick, S. Khan, L. M. Frost, N. J. Smith, S. Cheung and G. Pairaudeau, *Tetrahedron*, 2000, **56**, 8953–8958.
35 C. Gatanaga, B. Yang, Y. Inadomi, K. Usui, C. Ota, T. Katayama, H. Suemune and M. Aso, *ACS Chem. Biol.*, 2016, **11**, 2216–2221.
36 C. Paolella, D. D'Alonzo, G. Palumbo and A. Guaragna, *Org. Biomol. Chem.*, 2013, **11**, 7825–7829.
37 R. Appel and H. Mayr, *J. Am. Chem. Soc.*, 2011, **133**, 8240–8251.
38 M. E. Belowich and J. F. Stoddart, *Chem. Soc. Rev.*, 2012, **41**, 2003–2024.
39 F. Li, Y. Zhang, J. Bai, M. M. Greenberg, Z. Xi and C. Zhou, *J. Am. Chem. Soc.*, 2017, **139**, 10617–10620.
40 J. Bai, Y. Zhang, Z. Xi, M. M. Greenberg and C. Zhou, *Chem. Res. Toxicol.*, 2018, **31**, 1364–1372.
41 A. Gennari, J. Wedgwood, E. Lallana, N. Francini and N. Tirelli, *Tetrahedron*, 2020, **76**, 131637.
42 C. Z. Zhou, J. T. Sczepanski and M. M. Greenberg, *J. Am. Chem. Soc.*, 2012, **134**, 16734–16741.
43 M. Ren, M. Shang, H. Wang, Z. Xi and C. Zhou, *Nucleic Acids Res.*, 2021, **49**, 257–268.
44 D. Vasudevan, E. Y. D. Chua and C. A. Davey, *J. Mol. Biol.*, 2010, **403**, 1–10.
45 A. Maiti and A. C. Drohat, *J. Biol. Chem.*, 2011, **286**, 35334–35338.
46 L. Zhang, X. Lu, J. Lu, H. Liang, Q. Dai, G.-L. Xu, C. Luo, H. Jiang and C. He, *Nat. Chem. Biol.*, 2012, **8**, 328–330.
47 B. O. Keller, J. Sui, A. B. Young and R. M. Whittal, *Anal. Chim. Acta*, 2008, **627**, 71–81.
48 K. Hodge, S. T. Have, L. Hutton and A. I. Lamond, *J. Proteomics*, 2013, **88**, 92–103.
49 B. Dubreuil, O. Matalon and E. D. Levy, *J. Mol. Biol.*, 2019, **431**, 4978–4992.
50 E. D. Levy, *J. Mol. Biol.*, 2010, **403**, 660–670.
51 J. Warwicker, S. Charonis and R. A. Curtis, *Mol. Pharm.*, 2014, **11**, 294–303.

© 2023 The Author(s). Published by the Royal Society of Chemistry